Circular Degree Hough Transform

Alejandro Flores-Mendez and Angeles Suarez-Cervantes

Universidad la Salle,
LIDETEA,
México D.F., México
aflores@ci.ulsa.mx, msuarez@lci.ulsa.mx
http://www.ci.ulsa.mx/~aflores

Abstract. The Circular Hough Transform (CHT) is probably the most widely used technique for detecting circular shapes within an image. This paper presents a novel variation of CHT which we call the Circular Degree Hough Transform (CDHT). The CDHT showed better performance than CHT for a number of experiments (eye localization, crater detection, etc.) included in this document. The improvement is mainly achieved by considering the orientation of the edges detected.

Keywords: Hough Transform, Circle Detection.

1 Introduction

One of the main problems in the image processing area refers to the detection of common shapes such as lines and circles. For this purpose, a number of techniques have been developed raging from very general ones to heuristical *ad hoc* algorithms [1]. Among the former, we can find the Hough Transform [2] which can detect analytically defined shapes. A decade after the appearance of the Hough Transform (HT), Duda and Hart [3] developed what nowadays is called the Generalized HT (GHT) which can be used to detect arbitray shapes not necessarily having a simple analytical form. From the GHT, a number of variations have been developed, specially for the case of circle detection [4], [5], [6], [7], [8] which is the case we are interested in this paper. Besides these variations, *Thresholding*, *Sliding Window*, etc. have been used for proper detection. These variations are necessary since only in scarce occasions the circular shape we want to detect in an image truly corresponds to a circle, and even if the image contains a circle it might not be complete. On the other hand, the number of applications that could benefit from the adequate detection of circular shapes count in great numbers. Some examples are crater detection[9], eye localization[10], RoboCup [11], just to name a few.

The current paper shows a novel method, which uses the information related to the edges of an image. In fact, this proposal uses the degree or orientation of the edges detected. However, instead of "tracing a line" into the accumulator in the direction related to the edges [7][1], we use these as a parameter to maximize the elements of the accumulator for which the likelihood between the ideal degree and the edges degree is attained.

[1] Which often causes problems, even for small degree errors.

E. Bayro-Corrochano and J.-O. Eklundh (Eds.): CIARP 2009, LNCS 5856, pp. 287–294, 2009.

The paper is organized as follows. Section 2 describes the proposed algorithm in detail. Section 3 presents some experimental results. In Section 4 the conclusions are included.

2 The Circular Degree Hough Transform

Before we detail how is it that the Circular Degree Hough Transform (CDHT) works, we will briefly summarize how is that the CHT does. Basically, the CHT algorithm obtains the edges of an image. From them, it calculates the *accumulator*, which is a matrix equivalent to the result of the correlation between these edges and a mask containing a circle. Thus, the accumulator holds evidence of the center coordinates where a circle of a given radius r could be.

Canny is commonly the selected technique to detect the edges of an image, because it is relatively immune to noise as it includes a Gaussian filter. Moreover, Canny gives a single response for a single edge. This is important when trying to locate a circular shape since this reduces spurious responses that could affect what is stored in the accumulator. Now, let `edges` be a vector whose elements are the coordinates of the edges detected. Then, the corresponding pseudocode for CHT follows:

```
CHT (edges, r, ang_dif)
1.  initialize (acum)
2.  for i  ←  1 to length [edges]
3.     (x, y)  ←  edges [i]
4.      α  ←  0
5.     repeat
6.          α  ←  α  + ang_dif
7.         a  ←  discretized (x - r  cos (α ))
8.         b  ←  discretized (y - r  sin (α ))
9.         if (range (a, b))
10.             acum [a, b] ++
11.     until  α  >  2 π
12. return acum
```

where `range(a,b)` determines if `a,b` are proper values to index the `acum` variable. Notice that the maximums of the accumulator are the best candidates to be the center of a circular shape. The process is depicted in Fig. 1.

A variation of this process compares the elements of `acum` against a threshold, θ to determine if a circle is really included in the image [2]. Yet another variation, increases the values of `acum` not only for `(a,b)`, but for a neighborhood of this coordinate. This variation is called *Sliding Window* and is commonly used when the circle in the image has suffer a transformation into a slightly eccentric ellipse.

A problem with these approaches is that they are highly sensitive to noise, since many spurious edges could be detected. Moreover, in some cases[9], the

[2] The circles detected will be those elements for which `acum` $> \theta$. For some cases, before the comparison, it is convenient to normalize `acum` to the range $[0, 1]$.

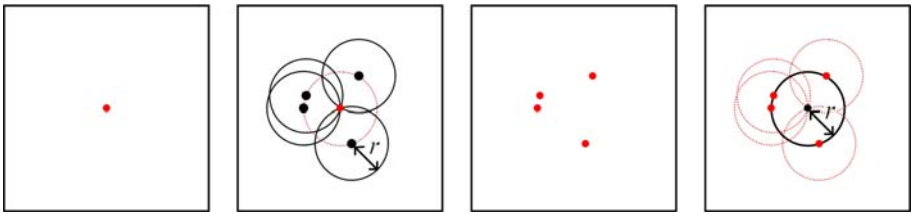

Fig. 1. (From left to right) 1) A point in an image 2) is used to determine if a circle of a given radius r contains it. This is stored in the accumulator (black points). 3) When the edges are calculated, the same process is done for every point on the image, 4) and the values of the accumulator (that hold the number of 'intersections') are used to determine the center of a circle with radius r within the image.

image itself contains features that are not noise, but will impact the edge detection process. In fact, if there are numerous edges not necessarily related to a circular shape, then the CHT could return a number of *false* detections. To avoid this, the image could be preprocessed by using some kind of filtering, but this is hardly useful if the edges are not noise related.

Pending on the application, a number of solutions could be helpful. For example, in iris detection, before the accumulator is increased, it could be checked that the edge separates a dark object of "adequate" dimensions surrounded by a bright object. Another modification could also consider the magnitude of the edges detected. The problem with these approaches is that they will be more noise resilient for some kinds of noise (even if no previous filtering is considered), but the numerous edges problem remains.

To solve this, it is possible to take into account the geometrical restrictions of the circular shapes. A simple manner to include this is to consider the angle of the edges. In fact, this was already explored [6], [7]. In these papers, the edge direction is used to "trace a line" along the direction of the edge detected, altering in this way the accumulator. In other words, these variations calculate the edges, obtain the directions associated to them, and increase the elements of the accumulator along the direction detected. The center of the circular shapes appearing on the image corresponds to those elements where the lines intersect (this process is depicted in Fig. 2). By doing this, if the image contains numerous edges, we still are able to correctly determine if a circular shape is included. However, the main problem with this approach is that an image is discrete; thus, the edge directions will include an error. Moreover, the circular shapes appearing on the image rarely correspond to a circle. This is particularly troublesome when trying to detect circular shapes with a "big" radius.

Our proposal still uses the edge directions. However, the difference is that it uses them to calculate an *error*, ϵ, between the ideal edge direction α and the real edge direction $\widehat{\alpha}$ as follows:

$$\epsilon\left(\alpha,\widehat{\alpha}\right)=\begin{cases}\left(|\alpha-\widehat{\alpha}|\right)/\pi & \text{if } |\alpha-\widehat{\alpha}|\leq\pi\\ \left(2\pi-|\alpha-\widehat{\alpha}|\right)/\pi & \text{otherwise}\end{cases}. \tag{1}$$

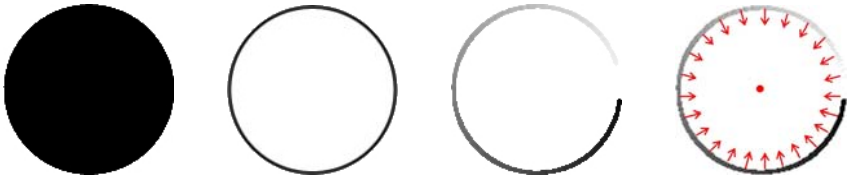

Fig. 2. (From left to right) 1) A circle. 2) The edges detected. 3) Degree of those edges (lighter elements are close to 0° while darker ones are closer to 360°). 4) By increasing the accumulator along the edge direction, the center of the circle is detected.

From this equation, the CHT is modified into the function `CDHT (edges, angles, r, ang_dif)`, and by adding between steps 4 and 5 the instruction:

4'. $\widehat{\alpha} \leftarrow$ `angles [i]`

where `angles [i]` holds the angle of `edges [i]`. Also, we substituted instruction in step 10 with:

10. `acum [a, b]` $\leftarrow$ `acum [a, b] + 1 -` ϵ $(\alpha, \widehat{\alpha})$

Different methods can be applied to obtain from an image its edges and their angles. For this proposal, the generalization of Sobel [12] was used. To define it, let $p, q \in \mathbb{Z}^{n+1}$, with:

$$p_i = c_{n,i-1}, \tag{2}$$

$$q_i = \begin{cases} c_{n,i} - c_{n,i-1} & \text{if } i < n/2 \\ -c_{n,i} + c_{n,i-1} & \text{if } i > n/2 \\ 0 & \text{otherwise} \end{cases}, \tag{3}$$

where $c_{n,k} := k!/\left(n!\,(n-k)!\right)$. From these two vectors, we obtain the template $T = pq^t$. T is used to calculate the magnitude of the edges of a grayscale image I in the x and y direction, denoted by M_x, M_y respectively, as:

$$M_x = I * T, M_y = I * T^t, \tag{4}$$

with $*$ denoting the $2D$ correlation. From M_x and M_y, the magnitude M is calculated as:

$$M = \sqrt{M_x^2 + M_y^2}, \tag{5}$$

while the direction of every pair $\left((M_x)_{i,j}, (M_y)_{i,j}\right)$ refers to the angle of this vector. From the magnitude, we define a edge as those pixels for which the magnitude is greater or equal to a threshold.

3 Experimental Results

To test the system, *CDHT* was implemented in MATLAB®. The implementation was used over three problems: 1) autocalibration, 2) detection in the presence of noise, and 3) detection of circular shapes with large unknown radii.

For the experiments, b denotes the edges coordinates of the input grayscale image, θ its associated directions, and the angle difference was set to one. From each image used for these experiments, the center coordinates $\widetilde{x}$ of those circular shapes appearing on it, as well as its radius $\widetilde{r}$, were experimentally determined. The coordinates of the circles detected by using $CDHT$, x^*, were compared by using the Euclidean norm over the difference $\Delta x := \widetilde{x} - x^*$, whilst for the radius, r^*, the absolute value of $\Delta r := \widetilde{r} - r^*$ was calculated.

3.1 Autocalibration

The autocalibration test consisted in presenting the system an image that contains a circular shape whose diameter is unknown. In this test, the system applies the $CDHT$ for a number of radii and selects the one for which the accumulator holds the greatest value; *i.e.*:

$$r^* = \arg\max \{\max \{CDHT\,(b, \theta, r, 1)\} : r \in \{r_{\min}, \ldots, r_{\max}\}\}\,. \tag{6}$$

In this particular case, $r_{\min} = 25, r_{\max} = 35$. On the other hand, x^* refers to the coordinates that hold the maximum value of $CDHT\,(b, \theta, r^*, 1)$ (the same was done for CHT).

The test was done over a set of sixty images of 320 by 240 from an eye captured in two different sessions with a web cam. The person was allowed to look into different directions. Because of this, the set was divided in two subsets. One containing 30 images for which the iris was about the middle of the eye[3]. The second subset contained the rest of the images[4]. For this subset, the radii difference was not calculated. The results are summarized in the next table.

Table 1. Results for the autocalibration test obtained through CHT and $CDHT$

	looking towards		looking away
	$mean\,(\|\Delta x\|_2)$	$mean\,(\|\Delta r\|)$	$mean\,(\|\Delta x\|_2)$
$CDHT$	0.8041	1.2667	1.6701
CHT	0.8834	1.0333	1.6121

Figure 3 shows some of the results attained during this test for $CDHT$.

3.2 Detection in the Presence of Noise

This test used the centered iris images subset. It is assumed that the radius r^* is already known. However, different kinds of noise (*Gaussian*, *Salt n' Pepper* and *Poisson*) were added to the images before determining the edges and their

[3] In these images the circular shape was closer to a circle

[4] These images contained circular shapes better described by an ellipse with greater eccentricities of those in the first set. This also explains the magnitued of the Δr

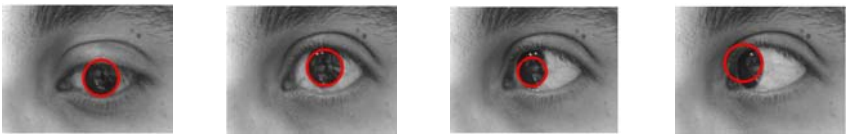

Fig. 3. Examples of the results obtained from the autocalibration test

magnitudes. Once this was done, the coordinates of $CDHT\,(b, \theta, r^*, 1)$ that hold its maximum value, x^*, are compared with the ideal, $\widetilde{x}$. If the euclidean norm of the difference Δx is less than or equal to $\sqrt{4}$, then the detection is qualified as *valid*, and *not valid* otherwise. For the process a Median Filter over a 5×5 window was used. The results of $CDHT$ and CHT are included in Table 2.

Table 2. Results for the circular shape detection in the presence of different kinds of noise

	Gauss, $\mu = 0, \sigma = 0.05$	*Gauss,* $\mu = 0, \sigma = 0.1$	*Salt n' Pepper*	*Poisson* $density = 0.1$
$CDHT$	83.33%	53.33%	100%	100%
CHT	100%	76.67%	100%	96.67%

3.3 Detection of Circular Shapes with Large Unknown Radii

One of the major problems of the CHT is the detection of circular shapes for a large radius. This problem follows from two major reasons: for large radii, the probability that the circular shape is perfect reduces considerably; the second reason, is that the probability to account a edge not related to a circular shape increases as a function of the radius. Consequently, the variations of the CHT that use the threshold and the direction of the edges for the detection seem like a natural alternative. However, since the edge direction variations "trace a line" in the direction of the edge detected, the accumulator rarely holds sufficient evidence of the circular shape for large radii. Clearly, this proposal is not affected by this matter, as it will increase the accumulator in a way proportional to how close the edge direction is to that expected.

To show this, a set of thirty satellite images of 256 by 256 from Mars containing craters of different sizes along with a number of other geographical features were used. For the test, no *a priori* information about the radii is assumed other than the range $r = \{15, 16, \ldots, 70\}$. The results of $CHT\,(b, \theta, r, 1)$ and $CDHT\,(b, \theta, r, 1)$ are compared to a threshold $th \in [0, 360]$. If the accumulator is greater or equal to th, then it is assumed that there is a circular shape for that particular location. Two selected elements were considered equivalent if the absolute difference between their center coordinates and their radius was for every element less than or equal to one. From this relation, the transitive closure was obtained, and the elements were clustered using this equivalence

relationship. This test produces two types of error: a False Rejection (FR) and a False Acceptance (FA)[5]. The selected values were compared with those of the ideals and were qualified as *valid* if the euclidean norm of the difference Δx is less than or equal to $\sqrt{4}$ and the absolute difference of Δr is less than or equal to 3. The selected values not fulfilling these requirements were qualified as a FR or a FA. For the detection, the edges deletion of selected circular shapes was done as proposed in [13].

Table 3. Results of the Large Unknown Radii Test. The cells contain the Valid Rate, FA Rate, FR Rate. If either, the FA or FR Rate are greater than 0.5, or the Valid Rate is less than 0.5 then the data is omitted.

th	360×0.2	360×0.25	360×0.3
$CDHT$	$(92.56\%, 32, 27\%, 11.37\%)$	$(85.83\%, 18.93\%, 17.46\%)$	$(74.91\%, 31.56\%, 28.65\%)$
CHT	–	$(81.25\%, 43.48\%, 27.43\%)$	$(71.88\%, 22.58\%, 31.85\%)$

Some results are included in Figure 4.

Fig. 4. Examples of the results obtained from the large unknown radii test. From left to right, original image, results obtained with the best threshold for CDHT and CHT. For the second and third image black and white circles represent FA and valid results respectively.

4 Conclusions

During this paper, we presented the CDHT. This variation of CHT calculates the data of the circular shapes appearing within an image with the same increasing the algorithm complexity, which is $\Theta(m)$, with $m = |\texttt{edges}|$.

For the Autocalibration Test, the results using both techniques were equivalent. This was to be expected, since only one circular shape in contained within every image, and it is clearly contrasted from the rest of the image.

For the Detection in the Presence of Noise Test, we also expected to obtain similar results for both techniques. However, CHT proved to be better for the Gaussian noise. The median filter was used since it is known that it preserves the edges of the filtered image. However, the square template altered the direction of the edges related to the iris. Thus, the recognition was not as good as desired.

[5] FA: if an existing crater is not detected. FR: If a not existing crater is detected.

The best performance of CDHT was obtained in the Large Unknown Radii Test. This is important, since this is the hardest test or the three proposed in this paper. Even more, this is probably the most likely scenario for practical applications. In this case, CDHT obtained the best ratios VR:FR and FR:FA.

References

1. Ayala-Ramirez, V., Garcia-Capulin, C.H., Perez-Garcia, A., Sanchez-Yanez, R.E.: Circle detection on images using genetic algorithms. Pattern Recognition Letters 27(6), 652–657 (2006)
2. Hough, P.V.C.: Methods and Means for Recognizing Complex Patterns. U.S. Patent 3, 069, 654 (1962)
3. Duda, R.O., Hart, P.E.: Use of the Hough Transformation to Detect Lines and Curves in Pictures. Comm. ACM 15, 11–15 (1972)
4. Kimme, C., Ballard, D., Sklansky, J.: Finding Circles by an Array of Accumulators. Communications of the ACM 18(2), 120–122 (1975)
5. Tsuji, S., Matsumoto, F.: Detection of ellipses by a modified Hough transformation. IEEE Transactions on Computers C-27(8), 777–781 (1978)
6. Xu, L., Oja, E., Kultanan, P.: A new curve detection method: randomized Hough transform (RHT). Pattern Recognition Letter 11(5), 331–338 (1990)
7. Aguado, A.S., Montiel, E., Nixon, M.S.: On Using Directional Information for Parameter Space Decomposition in Ellipse Detection. Pattern Recognition 28(3), 369–381 (1996)
8. McLaughlin, R., Alder, M.: The Hough transform versus UpWrite. IEEE Trans, PAMI 20(4), 396–400 (1998)
9. Salamuniccar, G., Loncaric, S.: Open framework for objective evaluation of crater detection algorithms with first test-field subsystem based on MOLA data. Advances in Space Research 42(1), 6–19 (2008)
10. Benn, D.E., Nixon, M.S., Carter, J.N.: Robust Eye Centre Extraction Using the Hough Transform. In: Bigün, J., Borgefors, G., Chollet, G. (eds.) AVBPA 1997. LNCS, vol. 1206, pp. 3–9. Springer, Heidelberg (1997)
11. Kaminka, G., Lima, P., Rojas, R. (eds.): RoboCup 2002. LNCS (LNAI), vol. 2752. Springer, Heidelberg (2003)
12. Nixon, M.S., Aguado, A.S.: Feature Extraction and Image Processing, 2nd edn. Academic Press, London (2007)
13. Flores-Méndez, A.: Crater Marking and Classification Using Computer Vision. In: Sanfeliu, A., Ruiz-Shulcloper, J. (eds.) CIARP 2003. LNCS, vol. 2905, pp. 79–86. Springer, Heidelberg (2003)